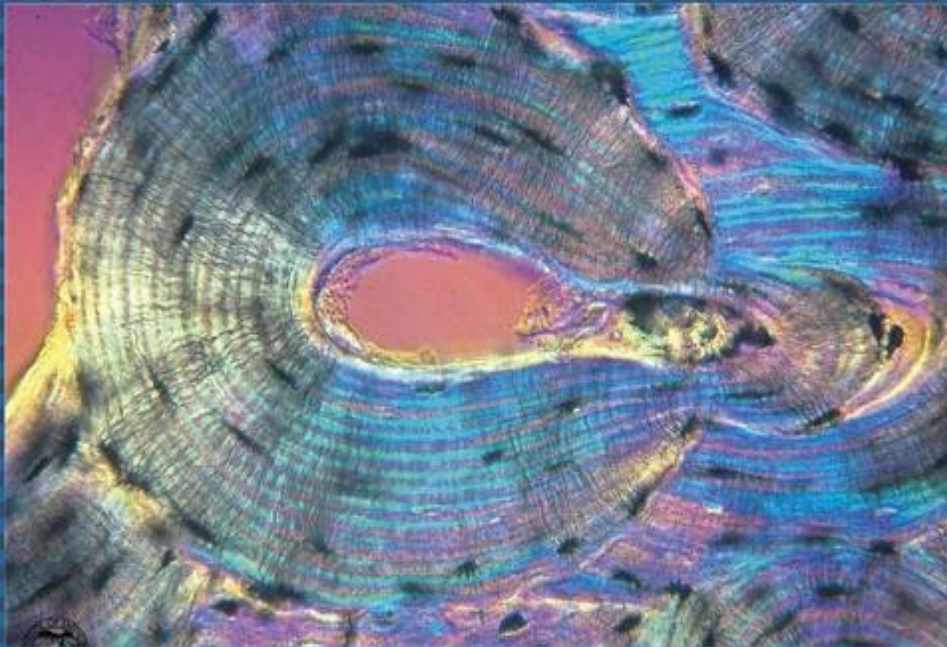




EGYPTIAN ACADEMIC JOURNAL OF
BIOLOGICAL SCIENCES
HISTOLOGY & HISTOCHEMISTRY

D



ISSN
2090-0775

WWW.EAJBS.EG.NET

Vol. 17 No. 2 (2025)



Comparative Study Between the Effect of Potassium Bromate and Calcium Carbonate on Stomach and Jejunal Mucosa of Adult Albino Rat (Histological & Immunohistochemical Study)

Asmaa S. Bassit and Dina M. Salah El Din

Department of anatomy & embryology, Faculty of medicine, Sohag university, Egypt.

E-mail : asmaabassit78@gmail.com

ARTICLE INFO

Article History

Received:22/7/2025

Accepted:7/9/2025

Available:11/9/2025

Keywords:

Potassium
bromate,
calcium
carbonate,
stomach,
jejunum.

ABSTRACT

Background: Potassium bromate serves as a chemical additive in food production, especially in bread making. Calcium carbonate is a supplement that has various industrial and pharmacological uses. **Aim of the work:** study the effect of Potassium Bromate and Calcium carbonate on stomach and jejunal mucosa of adult albino rat. **Material & methods:** 40 rats were subdivided into four groups: Group I (control group): rats were given distilled water, Group II: rats were given KBrO_3 (100 mg/kg/day,) dissolved in distilled water using a gastric tube for 4 weeks. Group III: rats were given calcium carbonate (CaCO_3) (1 g/kg/day) dissolved in distilled water using a gastric tube for 4 weeks. Group IV: rats were given both calcium carbonate (CaCO_3) and KBrO_3 . animals were sacrificed, and stomach and jejunum were isolated and subjected to stain with hematoxylin and eosin and immunohistochemical stain Ki67. **Result:** In KBrO_3 group, gastric mucosa was damaged in the form of deep gastric ulcers reaching muscularis mucosa, detachment of surface epithelial and destruction of parietal and chief cells. jejunal mucosa destructed with vacuolated villi epithelium and destroyed lamina propria, in CaCO_3 group jejunal & gastric mucosa had preserved architecture, in KBrO_3 & CaCO_3 there was some destruction in the gastric and jejunal mucosa. immunohistochemical result there was significant increase in Ki67 expression in KBrO_3 group and KBrO_3 & CaCO_3 group compared to control and CaCO_3 group. **Conclusion:** The current study demonstrates that potassium bromates had toxic effects on gastric and jejunal tissues, while calcium carbonate showed a comparatively protective role.

INTRODUCTION

Potassium bromate (KBrO_3) is a white crystalline compound widely used in the food industry, particularly in bread production, owing to its low cost and broad availability (Shanmugavel *et al.*, 2020). Several studies reported serious destructive effect of KBrO_3 on different organs such as the kidney, liver, thyroid gland, and the central nervous system (Ali *et al.*, 2018; Altoom *et al.*, 2018). The toxic effect of KBrO_3 has been mainly linked to excessive generation of ROS and free radicals. Once formed, these reactive species attack proteins, lipids, and nucleic acids, triggering oxidative stress, impairing cellular functions, and disturbing overall homeostasis, which eventually culminates in tissue injury." (Mubarak *et al.*, 2020). "As a strong oxidizing agent, bromate elevates hydrogen peroxide levels, promotes protein and lipid peroxidation, and suppresses antioxidant defenses, ultimately leading to oxidative stress (Ahmad and Mahmood, 2016).

In addition, bromate directly induces DNA strand breaks and mutagenic changes, which explains why its use has been prohibited in food manufacturing by several countries (Ahmad *et al.*, 2015; Chauhan and Jain, 2016). One of the adverse effects associated with KBrO_3 use is gastrointestinal irritation, which may present as vomiting, reduced appetite, excessive thirst, frequent urination, and constipation (Shanmugavel *et al.*, 2020).

Some research reported that KBrO_3 affected gastric mucosa through inflammation and necrosis and even ulcer formation, which led to bleeding and perforation in the stomach wall (Ali *et al.*, 2023). Calcium carbonate (CaCO_3) is an inorganic salt extensively utilized in therapeutic applications, including its role as a food additive, nutritional supplement, antacid, and phosphate-binding agent. Naturally, it is present in several biological sources, such as eggshells, oyster shells, the exoskeletons of crustaceans, and dark green vegetables like broccoli and kale (Al Omari *et al.*, 2016).

In addition to its therapeutic applications, calcium carbonate has various industrial uses such as paint, paper, adhesives, and fire extinguishers. It is also used in the composition of agricultural and mining dust, household cleaning agents, food colorants, and is incorporated into the formulation of cosmetic products (Foran *et al.*, 2013). It is commonly used as a calcium supplement to manage hypocalcemia, as an antacid for relieving gastrointestinal disorders, and as a phosphate binder in patients with chronic kidney disease (Fritz *et al.*, 2023). It exerts its pharmacological effects through three distinct mechanisms involving the stomach, small intestine, and bloodstream. Upon reaching the stomach, it dissociates into calcium ions (Ca^{2+}) and carbonate ions (CO_3^{2-}). The carbonate component interacts with free hydrogen ions (H^+), reducing their

concentration and thereby raising the gastric pH. This elevation in pH inhibits the activity of pepsin, bile acids, and toxins produced by *Helicobacter pylori* (Buchowski, 2015).

The inhibition of pepsin by CaCO_3 helps reduce mucosal damage and promotes the healing of gastric ulcers; however, some criticism remains regarding the ulcer-healing effects of calcium carbonate (Xu *et al.*, 2023).

The antacid effect of calcium carbonate not only neutralizes gastric acid but also promotes gastrointestinal motility by stimulating esophageal peristalsis, thereby facilitating acid clearance into the stomach and alleviating symptoms of heartburn (Garg *et al.*, 2022). While the toxicological effects of KBrO_3 and the therapeutic applications of CaCO_3 on the gastrointestinal system have been separately documented, their direct comparison remains insufficiently explored. Therefore, the present study was designed to investigate the ulcerogenic and oxidative effects of KBrO_3 and the potential gastroprotective role of CaCO_3 .

This experiment aimed to study the effect of Potassium Bromate and Calcium carbonate on stomach and jejunal mucosa of adult albino rats.

MATERIALS AND METHODS

Chemical:

Potassium bromate (KBrO_3): It is available as white crystals, which were obtained from a local chemical supplier, High Lab, Assuit, Egypt.

Calcium carbonate CaCO_3 : It is available as white crystals, which were obtained from a local chemical supplier, High Lab, Assuit, Egypt.

Animals:

Forty adult male albino rats (150–180 g) were utilized in this study. They were acquired from the Animal House of the Faculty of Medicine, Sohag University. The animals were maintained in four stainless steel cages under controlled, well-ventilated conditions. Standard laboratory diet and water were

provided. Proper sanitation and care were ensured to preserve the animal. All experimental protocols were approved by the Institutional Animal Ethics Committee of Sohag University's Experimental Animal Research Laboratory."

The animals were subdivided into four groups:

Control group: rats were given distilled water.

KBrO₃ group: rats were given KBrO₃ at a dose of 100 mg/kg/day dissolved in distilled water using a gastric tube for 4 weeks (Altoom *et al.*, 2018).

CaCO₃ group: rats were given calcium carbonate (CaCO₃) at a dose of 1 g/kg/day dissolved in distilled water using a gastric tube for 4 weeks (Stojiljkovic *et al.*, 2012)

KBrO₃&CaCO₃ group: rats were given calcium carbonate (CaCO₃) at a dose of 1 g/kg/day and KBrO₃ at a dose of 100 mg/kg/day dissolved in distilled water using a gastric tube for 4 weeks.

Methods:

Scarification was performed 24 hours after the final dose. They were anesthetized by intramuscular injection of a mixture of Ketamine (90 mg/kg body weight) and Xylazine (10 mg/kg body weight).

For each group, animals' organs were isolated carefully under the dissecting microscope.

Tissue specimens were initially fixed in 10% formalin solution for 24–48 hours, after which they were transferred to 70% ethanol for storage until processing for histological sectioning.

The histological changes in the stomach and jejunum were examined by:

(1) Light microscopy:

The specimens were fragmented, ranging from 0.5-1cm, and fixed with 10% formalin and then stained with haematoxylin and eosin.

(2) Immunohistochemical staining:

Antigen retrieval was performed by heating the tissue sections in 10 mM citrate buffer (AP9003), pH 6.0, for 10 minutes. Subsequently, the sections were

incubated for one hour with the antibodies.

- **Ki-67** (marker of proliferation Kiel 67): a protein that serves as a marker for cell proliferation, primarily used in cancer diagnosis and prognosis. It's found in the cell nucleus during active phases of the cell cycle (G1, S, G2, and mitosis), but not in resting (G0) cells. A higher Ki67 level generally indicates a faster-growing tumor and may suggest a poorer prognosis, tonsil tissue was used as a positive control due to its high proliferative activity, whereas negative controls were prepared by processing the same tissue samples without the primary antibody, nuclear staining with brown coloration consider positive reaction (Ko *et al.*, 2017; Peng *et al.*, 2024).

Morphometric Study:

The body weight was measured individually for each animal at the start (initial body weight) and at the end (final body weight) of the experimental period. These measurements were used to evaluate weight changes across different groups.

Quantitative analysis was conducted by selecting 10 non-overlapping fields from each section. Measurements were carried out using ImageJ software (version 1.51k; Wayne Rasband, NIH, USA). The results were collected from H&E and immunohistochemical sections. The following parameters were calculated for quantitative evaluation:

1-Assessment of gastric mucosal lesion (ulcer index) in H&E section:

Gastric ulcers were examined and quantified with the aid of a magnifying glass. The severity of each lesion was scored based on the following criteria (Sabiua, 2015; Abd El-Naeem, 2022) as follows:

Score 0: Normal mucosal color.

Score 0.5: Presence of reddish discoloration.

Score 1.0: Pinpoint (spot) ulcers.

Score 1.5: Small ulcers with visible hemorrhage.

Score 2.0: Deep ulcerations.

Score 3.0: Evident perforations.

The Ulcer Index was determined using the equation: (Ahmed *et al.*, 2022)

Ulcer Index = UN + US + (UP × 0.1),
where:

UN = Mean number of ulcers per rat

US = Mean severity score

UP = Proportion (%) of rats with ulcers.

2- The total mucosal thickness of jejunum was measured from the apex of the villus to the muscularis mucosae using H&E-stained sections at 100X magnification (Bahey and Elswaidy, 2021).

3- Area percentage of Ki67 expression in Ki67-immune-staining section of stomach and jejunum at 100X magnification.

Statistical Analysis:

The collected data were statistically analyzed using Student's t-test and analysis of variance (ANOVA), followed by turkeys post hoc test comparisons to detect intergroup differences. The significance of variations in each measured parameter, compared to the control group, was determined based on the P-value. All values were expressed as mean ± standard deviation (SD). Statistical analysis was performed using SPSS software, version 17.0 (SPSS Inc., Illinois, USA). A P-value less than 0.05 was considered statistically significant, whereas values greater than 0.05 indicated no significant difference.

RESULTS

Histopathological Result:

Stomach: In the control group, fundic mucosa appeared normal, formed of surface epithelium, lamina propria & muscularis mucosa. The lining epithelium had a high columnar lining composed of pale cytoplasm and oval nuclei located near the base of the cells. Tubular fundic glands were seen within the lamina propria, oriented perpendicularly to the surface (Fig.1A). Each gland showed three distinct regions: an upper isthmus that opened into the gastric pits; a neck region lined by mucous-secreting cells exhibiting pale cytoplasm and flattened basal nuclei, along with some pyramidal

parietal cells showing deeply acidophilic cytoplasm and centrally located vesicular nuclei (Fig.2B). a basal portion containing both parietal cells and chief cells, the latter displaying basophilic cytoplasm and rounded basal vesicular nuclei (Fig.1C).

In KBrO₃-treated group severe ulcerative lesions in the mucosa extending into the muscularis mucosa and alteration of the normal glandular structural organization also shedding and detachment of surface epithelial cells were evident, moreover there was destructed area within the basal part of the gland (Fig.2A), the epithelium covered surface was transformed from columnar to flattened epithelial cells, areas of extravasation of blood appeared, some parietal cells appeared with vacuolated cytoplasm and shrunken nuclei (Fig.2B), in the basal part parietal cell appeared vacuolated while others appeared swollen, while some chief cells appeared with darkly stained nuclei and vacuolated cytoplasm (Fig.2C).

CaCO₃-treated group gastric mucosa appeared near the normal except area of extravasation of the blood, area of destruction in the basal part of gastric gland (Fig. 3A), surface epithelium normal lined with columnar epithelium, except area of blood extravasation, the parietal cells appeared normal exhibiting round vesicular nuclei situated at the center and acidophilic cytoplasm (Fig. 3B), lower part of the gland partial appeared near normal and chief cells appeared normal except some which had vacuolated cytoplasm and shrunken nucleus (Fig.3C). In KBrO₃ & CaCO₃-treated group, gastric mucosa shows ulcer reaching the neck of the gland; also, there was erosion in surface epithelium (Fig.4A). Upper part of gland had wide gastric pit, area of blood extravasation, and some parietal cells was vacuolated with shrunken nuclei. Also, there was destruction and severe dilation in the basal part of the gastric gland. Vacuolated chief cells with intensely stained nuclei were observed (Fig. 4B, C).

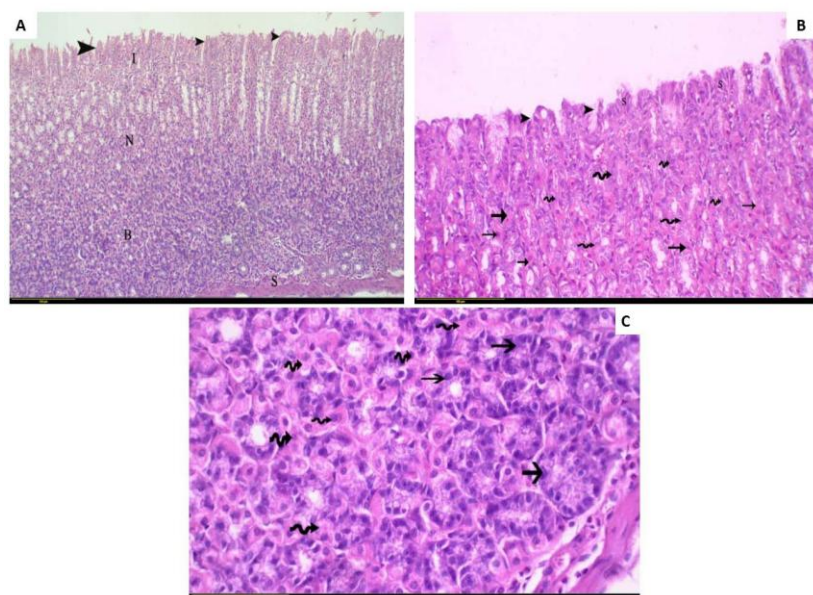


Fig. 1: H&E section in the gastric mucosa of control group. (A) Normal mucosa is composed of gastric gland resting in submucosal layer (S), the gastric gland composed of basal part (B), neck (N), and isthmus (I) open in the surface by gastric pit (arrowhead). (B): upper part of gland lined with single layer of columnar cell (S) ending by opening on surface by gastric pit (arrowhead), neck area formed of mucus neck cells (irregular arrow) & Parietal cells (arrow). (C): basal part of the fundic glands formed from parietal cell (irregular arrow), and chief cell (arrow). ($\times 100$, scale bar=150 μm & $\times 200$, scale bar=100 μm . & $\times 400$, scale bar=50 μm).

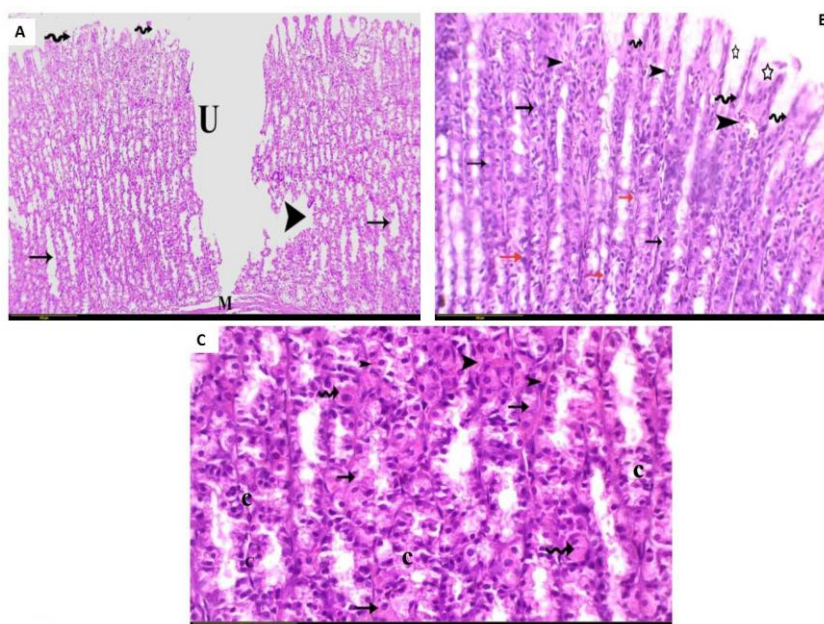


Fig. 2: H&E section in the gastric mucosa KBrO₃-treated group. (A): show ulcer (U) extended to mucosa of stomach (M), area of sloughed surface epithelium (irregular arrow), area of destruction within the basal part of the gland (arrowhead), fundic gland with wide lumen (arrow). (B): upper part of fundic gland with wide gastric pit (white star), flattened epithelial cells (irregular arrow), area of blood extravasation (arrowhead), partial (dark arrow), chief cells (red arrow) appear vacuolated. (C): lower part of gland, area of blood extravasation (arrowhead), some partial cells appear with vacuolated cytoplasm (arrow), other appear swollen (irregular arrow), chief cells appear with vacuolated cytoplasm and darkly stain nuclei (C). ($\times 100$, scale bar=150 μm & $\times 200$, scale bar=100 μm . & $\times 400$, scale bar=50 μm).

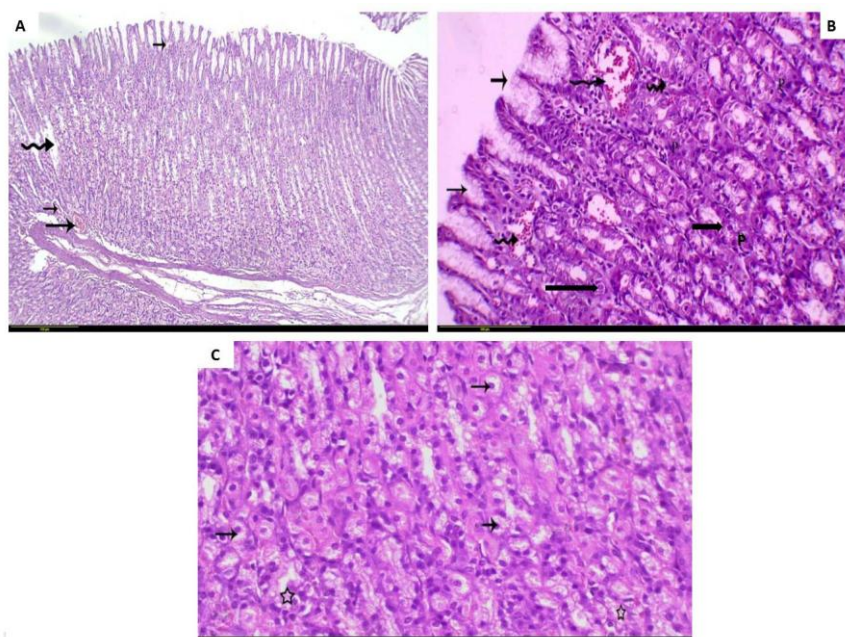


Fig. 3: H&E section in gastric mucosa of CaCO_3 - treated group, (A), which appears normal except area of extravasation of the blood (arrow) and areas of destroyed gastric gland (irregular arrow). (B) Upper part of gland appears normal, open with gastric pit (short arrow), there is an area of blood extravasation (irregular arrow), and parietal cells appear normal (long arrow). (C): lower part of gland, partial cells appear normal (arrow), also chief cells appear normal except some that appear with vacuolated cytoplasm and dark-stained nucleus (star). ($\times 100$, scale bar= $150\ \mu\text{m}$ & $\times 200$, scale bar= $100\ \mu\text{m}$. & $\times 400$, scale bar= $50\ \mu\text{m}$).

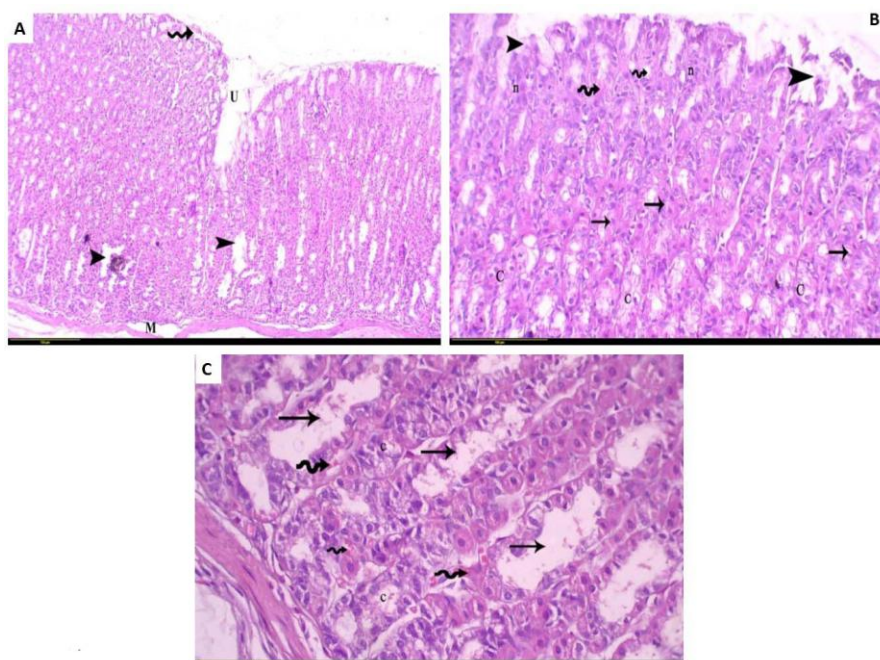


Fig. 4: H&E section in the gastric mucosa of CaCO_3 & KBrO_3 -treated group. (A): small superficial ulcer (U), erosion in superficial epithelium (irregular arrow), destruction and dilation in the basal part of the gland. (B, C) Upper part & lower part of gland, show destruction in the surface epithelium (arrowhead), extravasation of blood (irregular arrow), some partially vacuolated with darkly stained nuclei (short arrow), chief cell severely destroyed with vacuolated cytoplasm (C), basal gland dilated with destroyed wall (long arrow). ($\times 100$, scale bar= $150\ \mu\text{m}$ & $\times 200$, scale bar= $100\ \mu\text{m}$. & $\times 400$, scale bar= $50\ \mu\text{m}$).

Jejunum:

In the control group, the jejunal wall exhibited the typical four histological layers: mucosa, submucosa, muscularis externa, and serosa. The mucosal layer displayed numerous villi and intestinal crypts. The villi were elongated, finger-like structures containing a connective tissue core, whereas the crypts (crypts of Lieberkühn) appeared as invaginations within the lamina propria, forming simple tubular glands. The surface of the villi was lined by tall columnar epithelial cells possessing basally located oval nuclei and eosinophilic cytoplasm, interspersed with goblet cells, which appeared as clear vacuolated spaces among the epithelial lining (Figs. 5A&6A).

In the KBrO_3 -treated group, the jejunum exhibited marked histopathological alterations indicative of cellular damage. The intestinal villi were distorted and showed extensive degeneration, including desquamation of the surface epithelial cells. The lamina propria core was severely damaged, and areas of crypt destruction were evident. Infiltration of inflammatory cells was observed between the intestinal crypts, with some crypts also displaying cytoplasmic vacuolation. The submucosal layer showed pronounced structural deterioration, characterized by reduced cellularity, while the muscularis

mucosa appeared notably thinned (Figs. 5B& 6B).

The jejunal tissue in the CaCO_3 -treated group demonstrated relatively preserved architecture, with many villi appearing well-organized and lined by simple columnar epithelium featuring basal oval nuclei and an apical brush border. The connective tissue core of most villi appeared intact, though occasional villi displayed cytoplasmic vacuolation within their cores. Intestinal crypts were generally preserved and appeared nearly normal, but some of them appeared vacuolated. In contrast, the submucosa showed focal areas of structural disruption and tissue loosening. While muscularis externa appeared thin (Figs. 5C&6C).

In the group co-treated with CaCO_3 and KBrO_3 , the jejunal architecture was markedly disrupted, with extensive damage observed in the villi. Many villi exhibited fragmentation and epithelial shedding, accompanied by notable tissue loss. Although a few villi retained their simple columnar epithelial lining with basal oval nuclei and apical brush borders, most were degenerated. The intestinal crypts displayed cytoplasmic vacuolation, and some crypt epithelial cells had deeply stained, pyknotic nuclei. Additionally, discontinuity and structural deterioration were evident in both the submucosal and muscularis externa layers (Figs. 5D&6D).

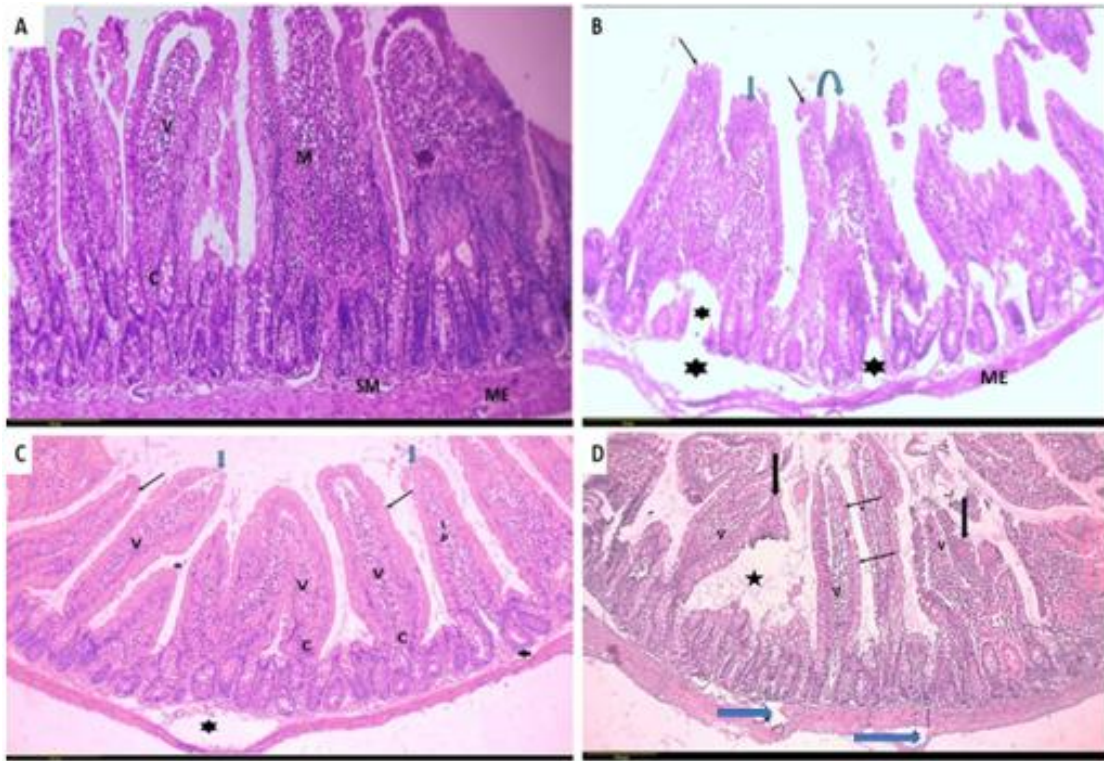


Fig. 5: H&E section in the jejunum. (A): control group showing mucosa (M) with finger-like villi (V) covered with simple columnar cells and simple tubular crypts in its lower part (c), normal submucosa (SM) and muscularis externa (ME). (B) Sections from the KBrO₃-treated group revealed markedly shortened and broadened intestinal villi (thick arrow), accompanied by epithelial discontinuity and desquamation (thin arrow). Evidence of villous fusion (curved arrow) was also apparent, along with severe structural damage to the crypt architecture and submucosal layer (star). Additionally, thinning of the muscularis externa (ME) was noted. (C): CaCO₃- treated group showing mucosa with well oriented villi (v) with a core of lamina propria (LP) and simple tubular crypts (C), villi showing normal simple columnar cells with basal oval nuclei and bearing a brush border (thin arrow) while others showing discontinuity and surface erosion of epithelial tissue (thick blue arrow). Submucosa (SM), muscularis externa (ME) showing areas of discontinuation and tissue loss (star). (D): CaCO₃& KBrO₃-treated group showing distortion of some villi (v) and destruction in the others (star), discontinuity and surface erosion of epithelial tissue (thick arrow). Some villi show regain of normal simple columnar cells with basal oval nuclei and apical surface bearing a brush border (thin arrow), while Submucosa (SM), muscularis externa (ME) show areas of destruction and tissue loss (blue arrow). (X100, scale bar=150 μ m).

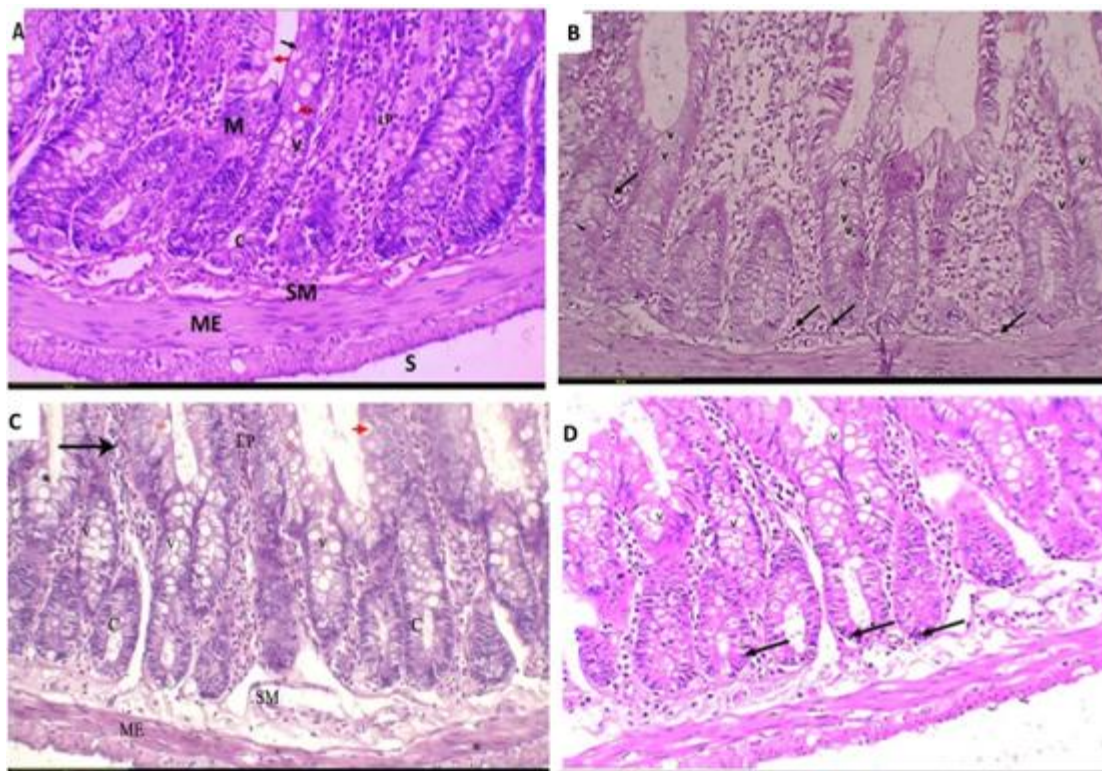


Fig. 6: H&E section in the jejunum at high magnification. (A) The control group demonstrated intact mucosa (M) with well-formed, elongated, finger-shaped villi (V) containing a central core of lamina propria (LP) and simple tubular crypts (c). The villi were lined by simple columnar epithelial cells with basally located oval nuclei and a distinct apical surface bearing a brush border (black arrow), interspersed with mucin-secreting goblet cells (red arrow). The submucosa (SM), muscularis externa (ME), and serosa (S) appeared normal and well-preserved. (B): KBrO_3 -treated group shows intestinal villi are severely destroyed with damaged lamina propria and multiple vacuolation within its covering epithelium. Some intestinal crypts appeared with cytoplasmic vacuolation (v), and there are inflammatory cells between crypts (thin arrow). (C): CaCO_3 -treated group in which intestinal villi were near normal, covered by columnar epithelium but some of them its lamina propria appears empty and vacuolated (arrow) also crypt (C) appears normal except some vacuolated (V), area of tissue loss of submucosa (SM) and thinning of muscularis mucosa (ME). (D): CaCO_3 & KBrO_3 treated group. There were distorted intestinal villi with destruction in the lining epithelium. The crypt epithelium exhibited cytoplasmic vacuolation along with deeply stained, pyknotic nuclei (thin arrow), and there was an area of tissue loss in the submucosa under the crypt. (x400, scale bar=50 μm).

Immune Histochemical Result (stain with Ki 67):

In Stomach:

In the control group, there was minimal reaction to Ki-67 immunostaining, which was visible as brown nuclear staining appeared at the isthmus part of the gastric gland & in submucosa (Fig.7A). While in the KBrO_3 -treated group, there was severe positive Ki-67 immunostaining reaction visible as brown nuclear staining in the

gastric mucosa (Fig.7B). CaCO_3 -treated group showed mild positive reaction to Ki-67 immunostaining, which was visible as brown in the gastric gland (Fig. 7C). In the KBrO_3 & CaCO_3 , severe positive Ki-67 immunostaining reaction was present through the gastric gland (Fig. 7D).

In Jejunum:

In the control group, there was minimal reaction to Ki-67 immunostaining, which was visible as

brown nuclear staining, predominantly localized in the basal region of the intestinal crypts. (Fig. 8A). While in the KBrO_3 -treated group, there was severe positive Ki-67 immunostaining reaction visible as brown nuclear staining in the intestinal crypts as well as the villi (Fig. 8B). CaCO_3 treated group showed mild positive reaction to Ki-67

immunostaining which was visible as brown nuclear staining in the intestinal crypts and as minimal reaction in the villi (Fig. 8C). In the KBrO_3 & CaCO_3 showed severe positive Ki-67 immunostaining reaction was visible as brown nuclear staining in the intestinal crypts as well as the villi (Fig. 8D).

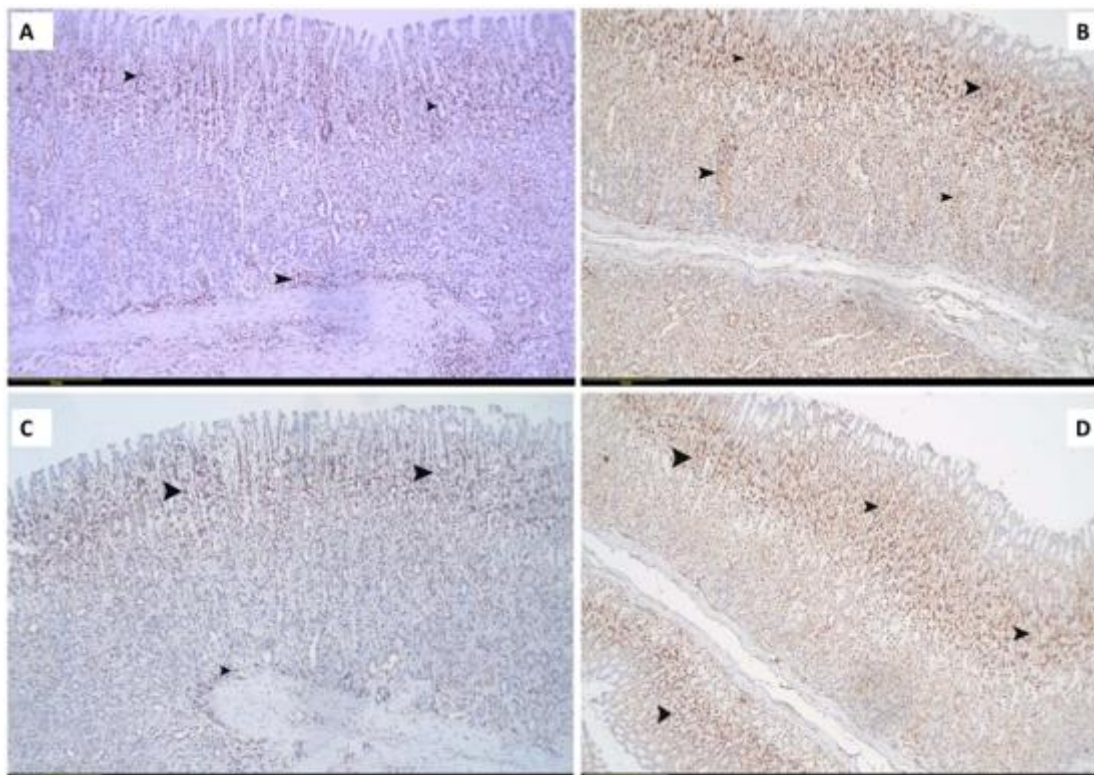


Fig. 7: A photomicrographic section in gastric mucosa. (A) Control group showing mild reaction to immunological stain Ki-67 appears in isthmus part of gland and submucosal layer (arrowhead). (B): KBrO_3 -treated group showing severe reaction to immunological stain Ki-67 (arrowhead). (C): CaCO_3 treated group showing mild reaction to immunological stain Ki-67 (arrowhead). (D): CaCO_3 & KBrO_3 treated group showing severe reaction to immunological stain Ki-67 (arrowhead). (ki67 \times 100 scale bar=150 μm).

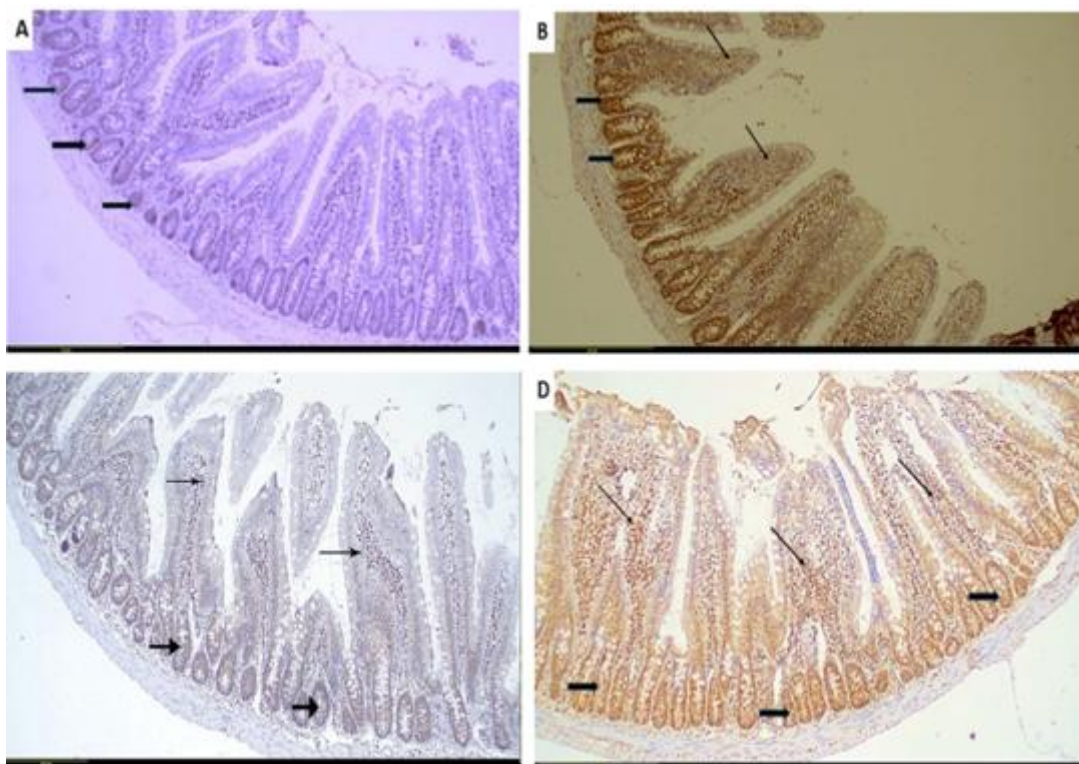


Fig. 8: A photomicrographic section in jejunum. (A): control group displays minimal Ki-67 immunostaining, which is visible as brown nuclear staining, localized in the basal region of the intestinal crypts (black arrows). (B): KBrO₃-group displays positive Ki-67 immunostaining which is visible as brown nuclear staining of the intestinal crypts (thick arrows), also it is abundant in the intestinal villi (thin arrows) (C): CaCO₃ group displays moderate reaction to Ki-67 immunostaining which is visible as brown nuclear staining of the intestinal crypts (thick arrows) and minimal reaction appears in the villi (thin arrows). (D): CaCO₃ group displays severe Positive Ki-67 immunostaining reaction, which is visible as brown nuclear staining of the intestinal crypts (thick arrows) and (thin arrows). (ki67x100 scale bar=150µm).

Morphometric Result:

General Observation (Body weight):

The average initial body weights of rats across all experimental groups showed no significant statistical variation. While at the end of the experiment, the mean of final body weight showed a significant decrease in

KBrO₃-treated group, followed by KBrO₃& CaCO₃, then CaCO₃, compared to the control group.

The mean of final body weight in CaCO₃ showed a significant increase when compared to the KBrO₃-treated group and KBrO₃& CaCO₃ group (Table 1).

Table 1: One-way ANOVA was used for comparative statistical analysis of the mean initial and final body weights among the different experimental groups of rats.

	Control group	KBrO ₃ group	CaCO ₃ group	KBrO ₃ & CaCO ₃ group	P value
Initial body weight	158.5±6.70	157.7±6.27	156±5.5	157.7±6.4	0.855
Final body weight	181±10.49	156±10.5 ↓	↑ 169.5±6.7 ↓	159.2±8.9 ↑	0.000

The value expresses as mean ± standard deviation.

↓ = significant decrease compared to all other group.

↓ = significant decrease compared to control group.

↑ = significant increase compared to KBrO₃ and KBrO₃& CaCO₃ group.

Ulcer Index in the Stomach:

There was a highly significant increase in the mean of ulcer index in KBrO_3 and KBrO_3 & CaCO_3 treated groups compared to the control group. There was a moderately significant increase between CaCO_3 and the control group. Also, there was a highly significant increase in ulcer index in KBrO_3 -treated group when compared with the KBrO_3 & CaCO_3 treated group. On the other hand, no significant difference in ulcer index between the

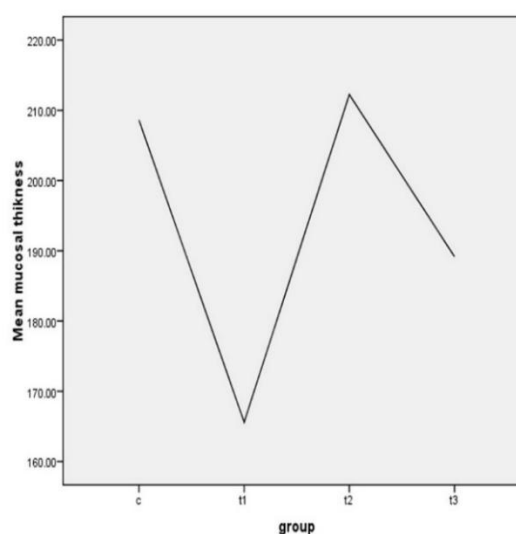
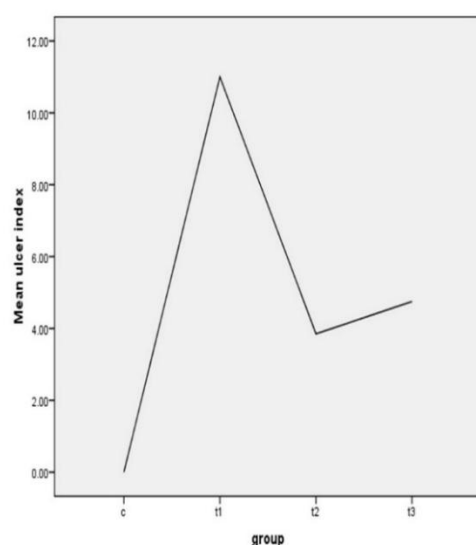
CaCO_3 and KBrO_3 & CaCO_3 treated groups. (Table 2, graph 1).

Mucosal Thickness of Jejunum:

A marked and statistically significant reduction in jejunal mucosal thickness was observed in the KBrO_3 -treated and KBrO_3 + CaCO_3 -treated groups compared to both the control and CaCO_3 -treated groups. No significant difference was detected between the CaCO_3 -treated group and the control group (Table 2, graph 1).

Table2: Mean values \pm SD of ulcer index (UI) in the stomach and jejunal mucosal thickness in different experimental groups where P1: difference between control group and KBrO_3 treated group, p2: difference between control group and CaCO_3 treated group, p3: difference between control group and KBrO_3 & CaCO_3 treated group, p4: difference between KBrO_3 treated group and CaCO_3 treated group, p5: difference between KBrO_3 treated group and KBrO_3 & CaCO_3 treated group, p6: difference between CaCO_3 treated group and KBrO_3 & CaCO_3 treated group

	Control group (c)	KBrO_3 Group(t1)	CaCO_3 Group(t2)	KBrO_3 & CaCO_3 Group(t3)	P value
Ulcer index In stomach	0 ± 0.00	11 ± 2.04	3.85 ± 4.12	4.75 ± 4.13	P1=0.000 P2=0.01 P3=0.002 P4=0.000 P5=0.000 P6=0.6
Mucosal thickness of jejunum	208.6 ± 16.03	106.5 ± 18.3	201.4 ± 13.7	109 ± 6.86	P1=0.000 P2=0.5 P3=0.002 P4=0.000 P5=0.001 P6=0.000



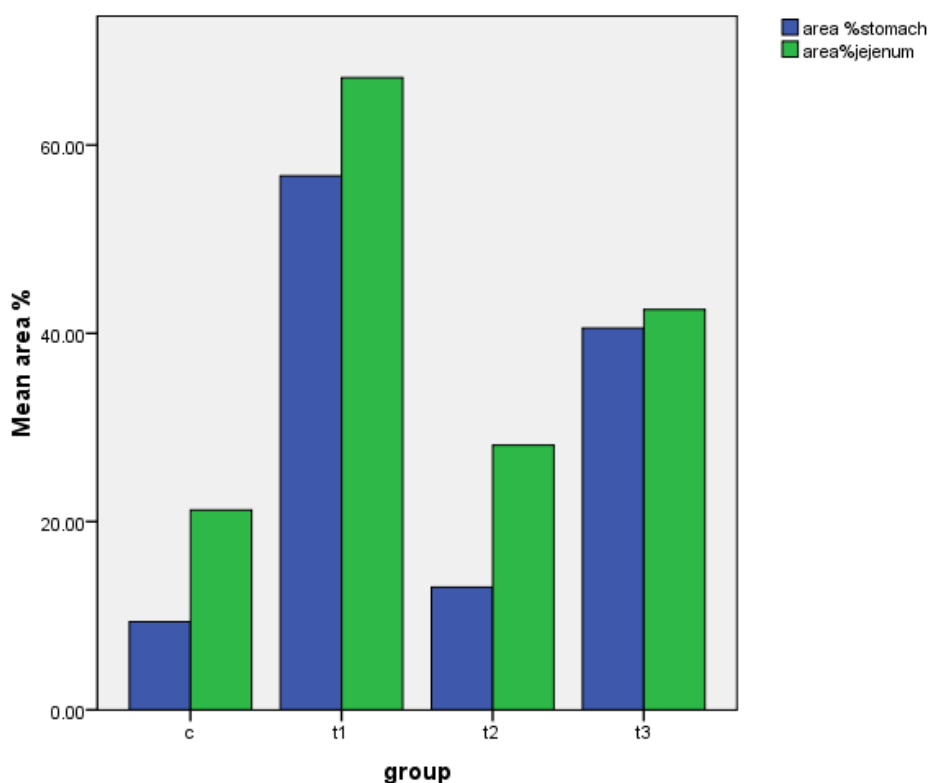
Graph (1): Mean values of ulcer index of stomach and jejunal mucosal thickness in different experimental group

Area% of Ki67 Expression in Stomach and Jejunum:

- A highly significant increase in the percentage area of Ki67 expression was observed in the gastric mucosa of both the KBrO_3 -treated and $\text{KBrO}_3 + \text{CaCO}_3$ -treated groups compared to the control group, while no significant difference was noted between the CaCO_3 -treated and control groups. Additionally, Ki67 expression was significantly higher in the KBrO_3 group compared to both the CaCO_3 and $\text{KBrO}_3 + \text{CaCO}_3$ groups. A significant increase was also detected in the $\text{KBrO}_3 + \text{CaCO}_3$ group relative to the CaCO_3 -treated group (Table 3, Histogram1).
- The percentage area of Ki67 expression in the jejunum was significantly increased in both the KBrO_3 -treated and $\text{KBrO}_3 + \text{CaCO}_3$ -treated groups compared to the control group. But a mild statistically significant difference was also noted between the CaCO_3 -treated group and the control group. Moreover, a significant elevation in Ki67 expression was observed in the KBrO_3 and $\text{KBrO}_3 + \text{CaCO}_3$ groups when compared to the CaCO_3 -treated group. (Table 3, Histogram1).

Table3: Mean values \pm SD of area % of Ki 67 immunohistochemical stain in the stomach & jejunum in different experimental groups.

	Control group(c)	KBrO_3 Group(t1)	CaCO_3 Group(t2)	KBrO_3 & CaCO_3 Group(t3)	P value
Area % of Ki67 in stomach	9.36 \pm 4.30	56.71 \pm 4.34	13.02 \pm 3.6	40.54 \pm 6.05	P1=0.000 P2=0.05 P3=0.000 P4=0.000 P5=0.000 P6=0.000
Area % of Ki67 in jejunum	21.2 \pm 4.02	67.1 \pm 5.6	28.12 \pm 6.2	42.5 \pm 3.8	P1=0.000 P2=0.01 P3=0.000 P4=0.000 P5=0.000 P6=0.000



Histogram 1: Area % of Ki 67 positive expression in the stomach and jejunum of different experimental groups.

DISCUSSION

Potassium bromate is a strong oxidizing agent commonly used as an effective and low-cost dough improver in the baking industry. Owing to its functional benefits, it plays a key role in enhancing the quality of bread. It influences various food biomolecules, particularly starch and proteins, by modifying gelatinization, viscosity, swelling behavior, and gluten structure, thereby improving the overall baking properties (El Ati-Hellal *et al.*, 2018). However, due to its toxicological risks, the use of potassium bromate as a food additive has been prohibited in many countries. The European Union has categorized it as a Group 1B carcinogenic substance, indicating its potential to cause cancer (Chauhan and Jain, 2016).

Calcium carbonate (CaCO_3) is the cheapest commercially available inorganic abundant mineral. It is extensively utilized as a filler in various industries, including paper, plastics, rubber, paints, and food products. Also, it's used as an antacid in heartburn,

essential for bone health and muscle function (Foran *et al.*, 2013).

In our study, we tried to make a comparative evaluation between the effect of KBrO_3 as a food additive and CaCO_3 as a supplementation on the stomach and jejunum.

In our study, there was a significant decrease in the final body weight in KBrO_3 and KBrO_3 & CaCO_3 -treated rats when compared to normal. This agrees with Rezaq, (2017) who approved that KBrO_3 treatment was associated with a significant decline in body weight among Swiss mice, and also with Radwan *et al.*, (2022) who noticed; a significant reduction in rats body weight following the administration of potassium bromate at a dose of 50 mg/kg; this attributed to toxic effect of KBrO_3 on the gastrointestinal tract where it cause oxidative stress (OS) and increase lipid peroxidation which lowers the activities of different enzymes in the brush border and villi of the intestine which affect process of digestion and absorption of food (Ahmad *et al.*, 2015).

In our research, histological results showed that in the stomach of KBrO_3 -treated group in the stomach, there were deep gastric ulcers reaching muscularis mucosa and distortion of the glandular histoarchitecture and destruction in partial cells and chief cells, which became vacuolated with dark-stained nuclei. On the other hand, the intestinal structure was markedly compromised. Villi appeared deformed, with evident desquamation and loss of epithelial integrity.

This result is in line with Ali *et al.* (2023), who found that use of KBrO_3 in a dose of 30 mg/kg for 8 weeks leads to destruction in the stomach mucosa in the form of vacuolation and apoptosis of peptic and parietal cells, also noticing an increased amount of collagen fiber between fundic glands. Bayomy *et al.* (2016) explained that degenerative changes of KBrO_3 were due to its oxidative stress role that led to mitochondrial damage and release of cytochrome-c into cytosol. Also, Salami *et al.* (2020) approved that the ulcerogenic effect of potassium bromate may be attributed to its ability to trigger inflammatory cell infiltration, stimulate oxidative stress, and activate the sodium-potassium ATPase; all of these contribute to the onset of gastritis and mucosal damage. Also, Al-Mareed *et al.*, (2022) said that potassium bromate (KBrO_3) interacts with tissue surfaces; it tends to cause structural disruption, where its reduction to bromide is associated with the generation of reactive oxygen species (ROS). These ROS contribute to cellular damage, including the degradation of biological membranes.

Also, Bahey and Elswaidy, (2021) revealed that the jejunal tissue of rats treated with KBrO_3 exhibited evident epithelial disruption along the villi, characterized by extensive cellular degeneration and detachment of both epithelial and goblet cells, Ahmad *et al.*, (2015) in rats treated with KBrO_3 the duodenal mucosa showed disorganization of its surface epithelium

and damage of its brush border with increase in inflammatory cells infiltration. Nazir *et al.* (2025) approved that KBrO_3 increases colon crypt thickening epithelium, and produces foci in the crypt, which are an indication of gastrointestinal preneoplastic lesion; Mohamed and Saddek. (2019) KBrO_3 exerts its toxic effects mainly through oxidative stress, which arises from an overproduction of reactive oxygen species (ROS), which interact with cellular lipids, proteins, and nucleic acids, ultimately causing structural and functional damage to the tissues of kidney and testis.

The KBrO_3 -treated group exhibited a significant increase in Ki67 expression compared to the control group. Presented in the stomach mucosa and jejunal mucosa of treated rats. Ki-67 is a well-established nuclear marker widely used in pathology to assess cellular proliferation. In the present study, the increased Ki-67 supports the regeneration of damaged epithelial and mucus-secreting cells, helping to rebuild the mucosal barrier and promote healing of the injured areas.

Saf *et al.* (2015) mention that there was a strong association between increased Ki-67 expression and inflammation, metaplasia, and atrophy in the intestinal mucosa. Also, Elwan and Ibrahim. (2019) said when the rats exposed to tartrazine, they found significant increase in the Ki 67 expression which indicate cell proliferation and this proliferative activity may be due to regeneration of the damaged epithelium cells, in addition to Ali *et al.*, (2023) found that increase expression of PCNA which is proliferative marker and indicator of cell proliferation in the gastric mucosa of rats exposed to KBrO_3 .

An elevated PCNA immunostaining was detected in the epithelial lining, connective tissue, and muscle layers, indicating its distribution across various tissue components of the tongue in rats exposed to potassium bromate (KBrO_3), indicating enhanced

cellular proliferation as a regeneration of damaged tissue in these regions. (Moubarak *et al.*, 2020). Also, administration of KBrO_3 causes extensive DNA fragmentation in intestinal cells, which leads to extensive damage to intestinal villi and crypts. (Ahmad *et al.*, 2015)

In the present study, in the calcium carbonate (CaCO_3) group, most gastric sections retained normal epithelial integrity, and the glandular architecture was largely preserved, with minimal evidence of tissue damage or inflammation and some areas of hemorrhage. Similarly, the jejunal villi appeared mostly intact, lined by simple columnar epithelial cells with clear brush borders, while intestinal crypts maintained near-normal morphology, while others were vacuolated. Also, in the section of Ki67 in the stomach and jejunum, there was a significant increase in Ki67 fraction area compared to the control group.

This agrees with Pegu. (2020), which illustrates the antacid mechanism of CaCO_3 , in which it neutralizes gastric acid by reacting with hydrochloric acid in the stomach to produce calcium chloride, water, and carbon dioxide. This reaction increases gastric pH, alleviates mucosal irritation, and forms the basis of its traditional use as one of the earliest treatments for peptic ulcers, which has been proven to be very successful. (Hamidah *et al.*, 2021).

Ugwuja *et al.*, (2021) In cases of lead exposure, calcium carbonate administration appears to be the most effective in reducing and preventing lead accumulation in body tissues. While the group co-treated with CaCO_3 and KBrO_3 , the gastric and jejunal mucosa there was some degree of destruction in the gastric gland and superficial few ulcer, also jejunum villi showed some degree of disruption and area of tissue loss in the muscularis mucosa but less than that in KBrO_3 treated group, also there was moderate significant increase in Ki67 expression when compared to KBrO_3 treated group and control group

which approved that combination of CaCO_3 with KBrO_3 produce some degree of protection. This come Sánchez-Virosta *et al.*., (2019) with Calcium administration may exert a protective effect against arsenic and other metal toxicities, by regulation oxidative and reducing the motility of the gastrointestinal tract to decrease absorption of metals, also Jung *et al.*, (2021) mention that CaCO_3 when in coated by other material as TA(tannic acid) to become tannylated calcium carbonate it became to be strong antacid, antioxidant, and anti-inflammatory material through suppression of the mRNA expression of pro-inflammatory mediators & cytokines and protect cell from (ROS reactive oxygen species). Calcium carbonate (CaCO_3) combats oxidative stress by buffering stomach acid, which prevents reactive oxygen species (ROS) formation and lipid peroxidation. (Guizzardi and Moine 2017).

CaCO_3 stabilizes cell membranes via Ca^{2+} interactions, reducing ROS permeability, and supports endogenous antioxidant enzymes (SOD, CAT, GPx). (Görlach *et al.*, 2015).

Conclusion:

The current study demonstrates that potassium bromates (KBrO_3), which were commonly used as a food additive, had marked toxic effects on both gastric and jejunal tissues. In contrast, calcium carbonate (CaCO_3) showed a comparatively protective role. These findings highlight the hazardous impact of KBrO_3 on gastrointestinal health.

Declarations:

Ethics Approval: All animal procedures were conducted according to the ethical guidelines of the Sohag University Committee for Animal Care and Use. Approval was granted under certificate number [Sohage-5-12-4/2024-04].

Conflict of Interest: The authors declare no conflict of interest.

Author Contribution: All authors contributed equally to the preparation of this manuscript.

authors have read and approved the final version for publication.

Data Availability Statement: All data supporting the findings of this study are included within the article.

Funding Information: This research received no external funding.

Acknowledgment: We acknowledge the support and the help presented by Faculty of Medicine, sohag University, Egypt where the study was carried out. We also thank all people who helped in collecting, processing of samples.

REFERENCE

- Abd El-Naeem, A. F. (2022). Effect of nicotine on the structure of gastric mucosa of adult male albino rats and the possible protective effect of royal jelly (light and scanning electron microscopic study). *Egyptian Journal of Histology*, 45(2), 404–415. DOI: 10.21608/EJH.2021.48094.1382.
- Ahmad, M. K., & Mahmood, R. (2016). Protective effect of taurine against potassium bromate-induced hemoglobin oxidation, oxidative stress, and impairment of antioxidant defense system in blood. *Environmental Toxicology*, 31(3), 304–313. DOI: 10.1002/tox.22045.
- Ahmad, M. K., Khan, A. A., Ali, S. N., & Mahmood, R. (2015). Chemoprotective effect of taurine on potassium bromate-induced DNA damage, DNA-protein cross-linking, and oxidative stress in rat intestine. *PLoS ONE*, 10(3), e0119137. <https://doi.org/10.1371/journal.pone.0119137>
- Ahmed, O., Nedi, T. and Yimer, E.M. (2022). Evaluation of anti-gastric ulcer activity of aqueous and 80% methanol leaf extracts of *Urtica simensis* in rats. *Metabolism Open*, 14, p.100172. <https://doi.org/10.1016/j.metop.2022.100172>.
- Al Omari, M. M. H., Rashid, I. S., Qinna, N. A., Jaber, A. M., & Badwan, A. A. (2016). Calcium carbonate. *Profiles of Drug Substances, Excipients and Related Methodology*, 41, 31–132. <https://doi.org/10.1016/bs.podrm.2015.11.003>
- Ali, A. F., Abdelaziz, S. A., & Omara, R. (2023). Histological and Immunohistochemical Study on the Effect of Potassium Bromate on Gastric Fundic Mucosa of Adult Male Albino Rats and the Possible Ameliorating Role of Riboflavin. *Egyptian Journal of Histology*, 46(2), 886–904. DOI: 10.21608/EJH.2022.112210.1616
- Ali, B. H., Za'abi, M. A., Karaca, T., Suleimani, Y. A., Al Balushi, K., Manoj, P., Ashique, M., & Nemmar, A. (2018). Potassium bromate-induced kidney damage in rats and the effect of gum acacia thereon. *American Journal of Translational Research*, 10(1), 126–137.
- Al-Mareed, A. A., Farah, M. A., Al-Anazi, K. M., Hailan, W. A., & Ali, M. A. (2022). Potassium bromate-induced oxidative stress, genotoxicity and cytotoxicity in the blood and liver cells of mice. *Mutation Research/Genetic Toxicology and Environmental Mutagenesis*, 878: 503481.
- Altoom, N. G., Ajarem, J., Allam, A. A., Maodaa, S. N., & Abdel-Maksoud, M. A. (2018). Deleterious effects of potassium bromate administration on renal and hepatic tissues of Swiss mice. *Saudi Journal of Biological Sciences*, 25(2), 278–284. <https://doi.org/10.1016/j.sjbs.2017.01.060>
- Bahey, N., & Elswaidy, N. (2021). Lycopene reduces potassium bromate-induced structural alterations in the jejunal mucosa of adult rats. *Egyptian Journal of Histology*, 44(4), 1036–1049. doi: 10.21608/EJH.2020.53466.1401
- Bayomy, N. A., Soliman, G. M., & Abdelaziz, E. Z. (2016). Effect of potassium bromate on the liver of

- adult male albino rat and a possible protective role of vitamin C: Histological, immunohistochemical, and biochemical study. *The Anatomical Record*, 299(9), 1256–1269. <https://doi.org/10.1002/ar.23386>
- Buchowski, M. S. (2015). Calcium. In V. R. Preedy (Ed.), *Calcium: Chemistry, Analysis, Function and Effects* (pp. 3–20). Royal Society of Chemistry.
- Chauhan, D., & Jain, P. (2016). A scientific study of genotoxic-carcinogenic impacts of Potassium Bromate as food additive on human health. *International Research Journal of Engineering and Technology*, 3(6), 1136–1139.
- El Ati-Hellal, M., Doggui, R., Krifa, Y., & El Ati, J. (2018). Potassium bromate as a food additive: A case study of Tunisian breads. *Environmental Science and Pollution Research*, 25(3), 2702–2706. <https://doi.org/10.1007/s11356-017-0712-9>
- Elwan, W. M., & Ibrahim, M. A. (2019). Effect of tartrazine on gastric mucosa and the possible role of recovery with or without riboflavin in adult male albino rat. *Egyptian Journal of Histology*, 42(2), 297–311. DOI: 10.21608/ejh.2019.6312.1043
- Foran, E., Weiner, S., & Fine, M. (2013). Biogenic fish-gut calcium carbonate is a stable amorphous phase in the gilt-head seabream, *Sparus aurata*. *Scientific Reports*, 3(1), 1700. <https://doi.org/10.1038/srep01700>
- Fritz, K., Taylor, K., & Parmar, M. (2023). Calcium Carbonate. In StatPearls [Internet]. Treasure Island (FL): StatPearls Publishing. PMID: 32965974.
- Garg, V., Narang, P., & Taneja, R. (2022). Antacids revisited: Review on contemporary facts and relevance for self-management. *Journal of International Medical Research*, 50(3), 03000605221086457. <https://doi.org/10.1177/0300060522108645>
- Görlach, A., Bertram, K., Hudecova, S., & Krizanová, O. (2015). Calcium and ROS: A mutual interplay. *Redox Biology*, 6, 260. <https://doi.org/10.1016/j.redox.2015.08.010>.
- Guizzardi, S., & Moine, L. (2017). Oxidative stress, antioxidants and intestinal calcium absorption. *World Journal of Gastroenterology*, 23(16), 2841. <https://doi.org/10.3748/wjg.v23.i16.2841>.
- Hamidah, N., Aprilia, L., Hidayah, A. N., & Sukmawati, I. (2021). Test content calcium carbonate (CaCO₃) on the shell of the golden snail (*Pomacea canaliculata*) as an antacid substance. *Indonesian Journal of Biology Education*, 4(2), 14–18.
- Jung, S.-Y., Hwang, H., Jo, H.-S., Choi, S., Kim, H.-J., Kim, S.-E., & Park, K. (2021). Tannylated calcium carbonate materials with antacid, anti-inflammatory, and antioxidant effects. *International Journal of Molecular Sciences*, 22(9), 4614. <https://doi.org/10.3390/ijms22094614>
- Ko, G. H., Go, S. I., Lee, W. S., Lee, J. H., Jeong, S. H., Lee, Y. J., Hong, S. C., & Ha, W. S. (2017). Prognostic impact of Ki-67 in patients with gastric cancer: The importance of depth of invasion and histologic differentiation. *Medicine*, 96(25), e7181. DOI:10.1097/MD.00000000000007181.
- Mohamed, E. A., & Saddek, E. A. (2019). The protective effect of taurine and/or vanillin against renal, testicular, and hematological alterations induced by potassium bromate toxicity in rats. *The Journal of Basic and Applied Zoology*,

- 80(3). <https://doi.org/10.1186/s41936-019-0078-5>
- Moubarak, H. S., Essawy, T. A., & Mohammed, S. S. (2020). Carcinogenic effect of potassium bromate on tongue of adult male albino rats. *Journal of Radiation Research and Applied Sciences*, 13(1), 121–131. <https://doi.org/10.1080/16878507.2020.1713584>
- Nazir, S., Ahmad, M. K., & Nazir, Z. U. (n.d.). (2025). Ascorbic acid modulates potassium bromate-induced oxidative damage to rat intestine. Available at SSRN 5269390. <http://dx.doi.org/10.2139/ssrn.5269390>
- Pegu, K. D. (2020). Pharmacology of antacids. *Southern African Journal of Anaesthesia and Analgesia*, 26(6), S133–S136.
- Peng, C., Xu, X., Ouyang, Y., Li, Y., Lu, N., Zhu, Y., & He, C. (2024). Spatial variation of the gastrointestinal microbiota in response to long-term administration of vonoprazan in mice with high risk of gastric cancer. *Helicobacter*, 29(4), e13117. <https://doi.org/10.1111/hel.13117>
- Radwan, S. A., El Wessemy, A. M., Abdel-Aziz, B. F., & Abdel-Baky, E. S. (2022). Study the protective effect of vitamin E against potassium bromate toxicity on some hematological, renal, and hepatic functions in male rats. *Bulletin of Pharmaceutical Sciences Assiut University*, 45(2), 903–913. DOI: 10.21608/bfsa.2022.271769.
- Rezq, A. A. (2017). Potential protective and ameliorative effects of sesame oil and jojoba oil against potassium bromate (KBrO₃)-induced oxidative stress in rats. *Journal of Studies and Searches of Specific Education*, 3(1, Part 1), 155–189. DOI:10.21608/JSEZU.2017.238352.
- Sabiua, S., Garuba, T., Sunmonuc, T., Ajani, E., Sulymana, A., Nuraina, I., & Balogun, A. (2015). Indomethacin-induced gastric ulceration in rats: Protective roles of Spondias mombin and Ficus exasperata. *Toxicology Reports*, 2, 261–267. <https://doi.org/10.1016/j.toxrep.2015.01.002>
- Saf, C., Gulcan, E. M., Ozkan, F., Saf, S. P. C., & Vitrinel, A. (2015). Assessment of p21, p53 expression, and Ki-67 proliferative activities in the gastric mucosa of children with Helicobacter pylori gastritis. *European Journal of Gastroenterology & Hepatology*, 27(2), 155–161. <https://doi.org/10.1016/j.jgeb.2011.05.008>
- Salami, A. T., Adebimpe, M. A., Olagoke, O. C., Iyiola, T. O., & Olaleye, S. B. (2020). Potassium bromate cytotoxicity in the Wistar rat model of chronic gastric ulcers: Possible reversal by protocatechuic acid. *Journal of Food Biochemistry*, 44(12), e13501. <https://doi.org/10.1111/jfbc.13501>
- Sánchez-Virosta, P., Espín, S., Ruiz, S., Stauffer, J., Kanerva, M., García-Fernández, A. J., & Eeva, T. (2019). Effects of calcium supplementation on oxidative status and oxidative damage in great tit nestlings inhabiting a metal-polluted area. *Environmental Research*, 171, 484–492. <https://doi.org/10.1016/j.envres.2019.01.047>
- Shanmugavel, V., Santhi, K. K., Kurup, A. H., Kalakandan, S., Anandharaj, A., & Rawson, A. (2020). Potassium bromate: Effects on bread components, health, environment and method of analysis: A review. *Food Chemistry*, 311, 125964. <https://doi.org/10.1016/j.foodchem.2019.125964>
- Stojiljkovic, N., Stojiljkovic, M., Mihailovic, D., Randjelovic, P., Ilic, S., Gocmanac-Ignjatovic, M., & Veljkovic, M. (2012).

- Beneficial effects of calcium oral coadministration in gentamicin-induced nephrotoxicity in rats. *Renal Failure*, 34(5), 622–627. <https://doi.org/10.3109/0886022X.2012.664809>.
- Ugwuaja, E. I., Ugwu, N. C., Erejuwa, O. O., & Ugwuja, P. I. (2021). Effect of oral calcium supplementation after lead exposure on blood lead levels and haematological parameters in albino rats. *Journal of Applied Sciences and Environmental Management*, 25(2), 12–24. <https://doi.org/10.4314/jasem.v25i2.2>.
- Xu, L., Du, X., Zhou, Y., Cao, X., Shen, Y., Zhu, H., & Huang, H. (2023). Polyaspartic acid-stabilized CaCO_3 -containing in situ hydrogel for protection and treatment of gastric ulcer. *Molecular Pharmaceutics*, 20(4), 2105–2118. doi: 10.1021/acs.molpharmaceut.2c01062.

ARABIC SUMMARY

دراسة مقارنة بين تأثير برومات البوتاسيوم وكربونات الكالسيوم على الغشاء المخاطي للمعدة والصائم في الجرذان البيضاء البالغة (دراسة نسيجية ومناعية نسيجية)

أسماء صبري باسط، ودينا محمد صلاح
قسم التشريخ الادمي والأجنة، كلية الطب جامعه سوهاج

المقدمة: تُعد برومات البوتاسيوم (KBrO_3) من الإضافات الغذائية الشائعة ومن أرخص المحسنات المستخدمة في صناعة الخبز. أما كربونات الكالسيوم (CaCO_3) فهي تُستخدم كمكمل غذائي ولها تطبيقات صناعية ودوائية متعددة.

هدف الدراسة: تقييم ومقارنة تأثير كل من برومات البوتاسيوم وكربونات الكالسيوم على الغشاء المخاطي للمعدة والصائم في الجرذان البيضاء البالغة.

المواد وطرق العمل: تم تقسيم أربعين جرذاً أبيض بالغاً بشكل عشوائي إلى أربع مجموعات: المجموعة الأولى: تلقت ماءً مقطراً.

المجموعة الثانية : تلقت برومات البوتاسيوم بجرعة 100 ملغم/كغم/يوم عن طريق أنبوب المعدة لمدة 4 أسابيع.

المجموعة الثالثة: تلقت كربونات الكالسيوم بجرعة 1 غرام/كغم/يوم عن طريق أنبوب المعدة لمدة 4 أسابيع.

المجموعة الرابعة: تلقت كلاً من برومات البوتاسيوم وكربونات الكالسيوم بنفس الجرعات ولمدة 4 أسابيع.

بعد انتهاء فترة العلاج، تم قتل الحيوانات وجمع عينات من المعدة والصائم، ثم صُبغت العينات بصبغة الهيماتوكسيلين والإوزين، وأجريت الدراسة المناعية باستخدام مؤشر Ki-67 لتقييم النشاط الانقسامى للخلايا.

النتائج: أظهرت مجموعة برومات البوتاسيوم تلفاً شديداً في الغشاء المخاطي للمعدة، تمثل في تقرحات عميقة تصل إلى العضلة المخاطية، وانفصال في الطبقة السطحية، وتحطم في الخلايا الجدارية والرئيسية. كما أظهر الصائم تغيرات مدمرة واضحة، منها فجوات في الخلايا المبطنة وتلف في الطبقة الخاصة. في المقابل، احتفظت مجموعة كالسيوم كاربونات بالتركيب النسيجي الطبيعي إلى حد كبير في كل من المعدة والصائم. أما مجموعة العلاج المزدوج فقد أظهرت تلفاً متوسطاً مع بعض الحفاظ على البنية. وأظهرت نتائج الصبغة المناعية Ki-67 زيادة ملحوظة في النشاط الانقسامى للخلايا في مجموعتي برومات البوتاسيوم والعلاج المزدوج مقارنة بالمجموعة الضابطة ومجموعة كالسيوم كاربونات.

الاستنتاج: تُظهر الدراسة أن برومات البوتاسيوم تُحدث تأثيرات سامة واضحة على أنسجة المعدة والصائم، بينما أظهرت كربونات الكالسيوم دوراً وقائياً نسبياً ضد هذه التأثيرات.